Available online at www.sciencedirect.com
ScienceDirect
C. R. Geoscience 341 (2009) 21–35
COMPTES RENDUS GEOSCIENCE
http://france.elsevier.com/direct/CRAS2A/

Surface geosciences (hydrology-hydrogeology)

Seawater intrusion and associated processes: Case of the Korba aquifer (Cap-Bon, Tunisia)

Lamia Kouzana [a,*], Abdallah Ben Mammou [a], Mennoubi Sfar Felfoul [b]

[a] *Laboratoire des ressources minérales et environnement, département de géologie, faculté des sciences de Tunis, université de Tunis El Manar, 2092 Tunis, Tunisia*

[b] *Institut national agronomique de Tunis, 43, avenue Charles-Nicolle, 1082 Tunis, Tunisia*

Received 27 September 2007; accepted after revision 26 September 2008
Available online 18 November 2008

Presented by Ghislain de Marsily

Abstract

It has been established that intensive agricultural activities, usually, increase the risk of groundwater quality degradation through high groundwater pumping rates. In fact, the uncontrolled groundwater extraction causes a modification of natural flow systems and induces seawater intrusion from the coast and causes the groundwater quality deterioration. The Korba aquifer is located in the North-East of Tunisia, where a semi-arid Mediterranean climate prevails. The dry season is pronounced and this aggravates the situation, given that the highest water demand usually coincides with the drought period (dry weather conditions). The principal aim of this study is to characterize the hydrochemistry of this coastal aquifer, identifying the main processes that occur in the system, and to determine the extent of marine intrusion in the aquifer. In order to achieve this aim, geophysical and chemical parameters were measured, such as vertical electrical soundings (VES), electrical conductivity, pH, temperature, anions and cations concentrations. The analytical results obtained in the hydrochemistry study were interpreted using ion correlations with chloride and SO_4^{2-}/Cl^- and Mg^{2+}/Ca^{2+} ratios, in conjunction with calculations of the ionic deviations and the saturation indexes. Saturation indexes are calculated with the PHREEQC 2.8 software used for mineral saturation modelling of the aquifer seawater-freshwater mixture. The high groundwater salinity anomaly observed in Diar El Hajjej, Garaet Sassi and Takelsa-Korba zones was explained by the presence of seawater intrusion in these areas. This hypothesis is based on high chloride concentrations, the inverse cation exchange reactions, and the lower piezometric level compared to sea level. ***To cite this article: L. Kouzana et al., C. R. Geoscience 341 (2009).***

Résumé

Intrusion marine et les processus associés : le cas de l'aquifère de Korba (Cap Bon, Tunisie). La nappe côtière du Plio-Quaternaire de la région de Korba a été très sollicitée par les agriculteurs, ce qui a engendré, probablement, une inversion du gradient hydraulique et, par conséquent, l'avancée du biseau salé. Cela se traduit par une évolution spatio-temporelle de la piézométrie et de la qualité chimique des eaux. L'intrusion marine est mise en évidence par des méthodes géo-électriques (sondages électriques verticaux de type Wenner) et par l'étude de la conductivité électrique et des éléments chimiques majeurs. Pour identifier les processus et les réactions chimiques qui gouvernent sa salinisation et déterminent la limite de l'intrusion marine, nous avons eu recours à l'interprétation des résultats en utilisant la corrélation des éléments majeurs avec les chlorures, la variation des rapports SO_4^{2-}/Cl^- et Mg^{2+}/Ca^{2+}, le calcul des écarts ioniques et des indices de saturation. Les indices de saturation sont calculés par le

* Corresponding author.
E-mail address: lamia.kouzana@laposte.net (L. Kouzana).

1631-0713/$ – see front matter
doi:10.1016/j.crte.2008.09.008

logiciel PHREEQC 2.8, utilisé pour la modélisation de l'état de saturation des minéraux à l'état de mélange eau douce–eau de mer dans un système aquifère. Les résultats de ces analyses montrent que les zones à fortes salinités de Diar el Hajej, Garaet Sassi et Tazerka-Korba sont contaminées par les eaux marines. L'intrusion d'eau marine est mise en évidence par les fortes teneurs en chlorures, par la présence des réactions d'échange cationiques inverse et par une piézométrie négative. ***Pour citer cet article : L. Kouzana et al., C. R. Geoscience 341 (2009).***

Keywords: Korba aquifer; Seawater intrusion; Hydrochemistry; PHREEQC 2.8 software; Ionic deviation; Saturation indexes; Model

Mots clés : Nappe côtière de Korba ; Intrusion marine ; Hydrochimie ; Logiciel PHREEQC ; Écarts ioniques ; Indices de saturation ; Modélisation

1. Introduction

The delicate exploitation of a coastal aquifer usually induces problems of quantity and quality [13]. Indeed, a prolonged drought can be the origin of the rupture of the seawater–freshwater interface equilibrium, which in turn may cause seawater intrusion [17,18]. This can be seen through the space-time evolution of piezometric heads and the water chemical quality of these aquifers. Tunisia, like all Mediterranean countries, has experienced considerable periods of drought during the last two decades. The resulting water deficit was compensated through an increased withdrawal from aquifers. However, aquifers close to coastal areas are the most threatened as they are marked by a very strong borehole density resulting from an intense overexploitation, and shown by an increase in the mineralization of their waters [10]. This constitutes a limiting factor for their use. In this work, we will try to demonstrate seawater intrusion and its extension in the Plio-Quaternary aquifer of Korba, a Tunisian aquifer which is very heavily exploited by farmers.

The main purpose of our hydrochemical study is to determine the spatial extension of the salinization and also to identify the origins and the mechanisms governing its contamination. This will be shown through the use of the chemical contents in conjunction with the different processes, which modify the water mixture characteristics [33]. This change is due to the absence of balance between the aquifer and the water mixture. Indeed, the carbonates and clays contribute in the dissolution and the precipitation of some minerals, with cation exchange, which acts in opposition to the changes caused by the marine intrusion. These processes are the principal factors modifying the geochemistry of the water salinized by the seawater intrusion [33].

2. Geographic and geologic situation

The study area, covering 430 km^2 [30], is located in northeastern Tunisia, within the eastern coastal Plain of Cap-Bon (Fig. 1). This aquifer is bounded to the south by Oued Boulidine, to the north by Oued Lebna, to the west by Jebel Abdeerahmen and to the east by the Mediterranean Sea.

The outcropping formations of the study area are represented by Mio-Plio-Quaternary sediments [5]. The lower part of the Middle Miocene corresponds to detrital deposits known as the Beglia Formation. The upper part is composed of lenticular sandstones and marls with lignite levels called the Saouaf Formation. In the study area, the Upper Miocene is absent. This is believed to have been caused by the widespread erosional activity due to the Miocene orogeny [14].

The trangressional marine Pliocene sediments were unconformably deposited on these folded and eroded formations. These deposits are mainly composed of sandstone-sand-marl alternations topped by sandstones and sand [11]. This facies changes laterally to argillaceous sands or to consolidated sandstones, more or less argillaceous.

The Quaternary deposits are usually composed of two units: the lower unit of marine facies corresponds to sandy limestone with molluscs indicating the maximum flooding surface (MFS) of the Tyrrhenian transgression. The upper unit is mainly composed of a continental facies [28] with the occurrence of oolitic limestone and coprolites or pelloïds. These deposits form, nowadays, coastal consolidated dunes built by wind following marine regression [7,28]. The old consolidated dunes cover the Tyrrhenian deposits [28]. The encrusted limestone extends over significant distances. They are very rich in calcite, silica, sometimes in gypsum and alumina and frequently coloured by iron salts. Finally, The Holocene deposits are formed by recent alluvia of Oued Chiba, by sebkhas deposits and current dunes and beaches.

3. Hydrogeology

The hydrogeological study of the Korba area shows that the Plio-Quaternary detrital deposits constitute a

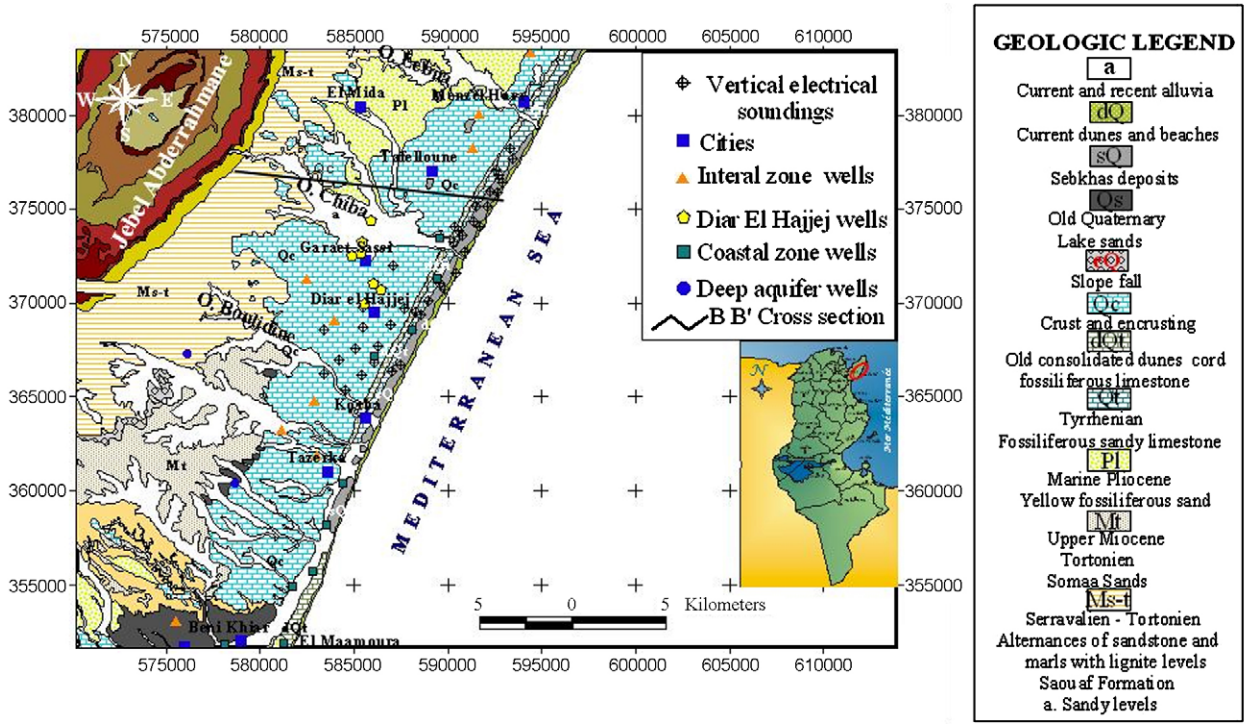

Fig. 1. Geology and samples and VES location in the Korba aquifer (June 2006).

Fig. 1. Localisation de la géologie de l'échantillonnage et des sondages électroniques verbiaux dans l'aquifère de Korba (juin 2006).

potential shallow aquifer. The marls of the Middle Miocene form the impermeable substratum of this aquifer [14] (Fig. 2).

The aquifer recharge is primarily made through the carved glacis rivers having a very porous lithology. The intercommunication between the Pliocene formations and recent alluvia is absent. The Quaternary recharge is increased partly by Pliocene sediments infiltration. Part of the groundwater flow occurs within the Tyrrhenian limestone before reaching the sea. Indeed, the Tyrrhenian deposits constitute a good reservoir and a key point of coastal aquifer recharge. Meteoric water recharge of the aquifer system is thought to occur through the coastal consolidated barriers, which characterize the Tyrrhenian beach. This contribution is shown through its great infiltration capacity and its role as topographic obstacle against surface run off. This helps water infiltration downstream in case it escapes infiltration upstream [14].

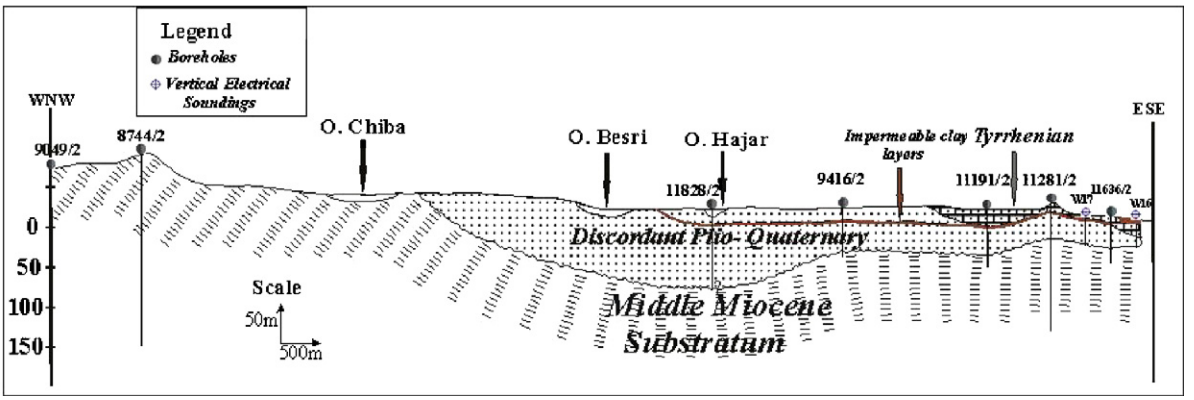

Fig. 2. Geological cross section B–B'.

Fig. 2. Coupe géologique B–B'.

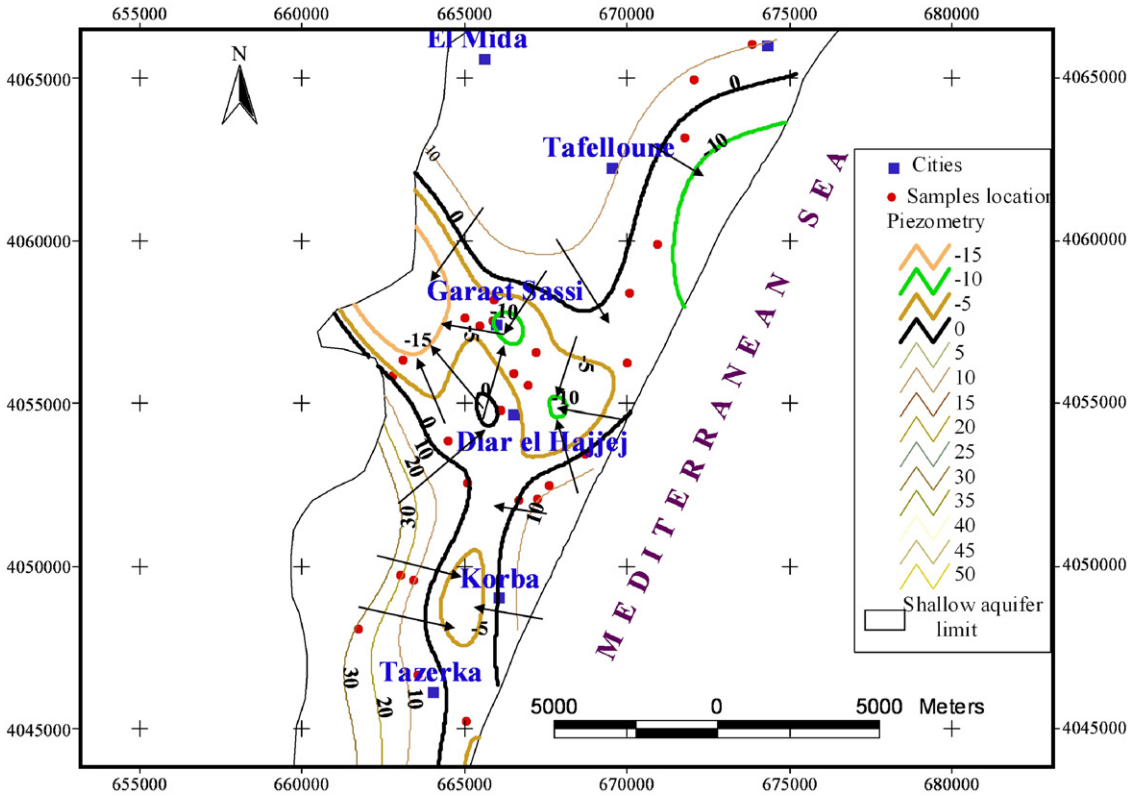

Fig. 3. Piezometric map of Korba aquifer (June 2006).

Fig. 3. Carte piézométrique de l'aquifère de Korba (juin 2006).

The recent 2006 piezometric map (Fig. 3) shows piezometric depressions related to overexploitation of the aquifer with negative piezometric levels on the order of −12 m. This map (Fig. 3) shows a multidirectional flow mainly oriented to the piezometric depressions located at Diar El Hajjej-Garaet Sassi and to the east of Tafelloune.

4. Methods

A multidisciplinary approach is needed in order to establish marine intrusion monitoring. Previous studies [3,4,9,12,19–21,23–25,29,32,33,35,36,38,41], through analytical, geophysical and modelling methods, have approached the problem and attempted to position the freshwater–seawater interface.

Other studies [1,15,20,22,26,27,34,38,39] defined the chemical processes and reactions, which characterize mineralization and would thus be responsible for groundwater chemical elements enrichment or impoverishment.

Geochemical properties were determined through different analyses, in order to characterize salinisation and the different factors monitoring its space-time evolution.

This article presents the analytical results of 28 samples, which were collected in June 2006. Twenty-six samples were collected from shallow wells and two were taken from the deep aquifer.

Electrical conductivity, temperature and pH were measured in situ. The cations (Na^+, K^+, Ca^{2+} and Mg^{2+}) were analysed at ''Laboratoire des resources minérales et environnement'' of the Faculty of Sciences of Tunis using Atomic Absorption Spectrometry. Bicarbonates were determined by the volumetric method, Cl^- was determined using the Mohr method and finally SO_4^{2-} was, spectrophotometrically, analysed.

The interpretation of the analytical results is shown numerically and graphically through the saturation index (SI), ionic deviations, Piper Diagram and binary diagrams.

SI and ionic deviations were calculated to better understand the hydrogeochemical processes that take place in the aquifer. Calculation of the ionic deviations (Δ) corresponds to a comparison of the measured concentration of each constituent to its theoretical

concentration of a known theoretical freshwater–seawater mixture calculated from the Cl concentration of the sample (see formula below) [16]:

$$\Delta C_i = C_{i,\,\text{sample}} - C_{i\,\text{mix}},$$

where ΔC_i is the ionic deviation of the ion i,

$C_{i,\,\text{sample}}$ is the measured concentration of the ion i in the sample, and $C_{i\,\text{mix}}$ is the theoretical concentration of the ion i for the theoretical (conservative) mixture of freshwater–seawater. The theoretical mixture concentrations were calculated taking into account seawater contribution (f_{sea}) based on the chloride contents in the sample ($C_{\text{Cl},\ \text{sample}}$), the freshwater Cl concentration ($C_{Cl,f}$) and the seawater Cl concentration ($C_{Cl,sea}$):

$$f_{\text{sea}} = \frac{(C_{Cl,\,\text{sample}} - C_{Cl,f})}{(C_{Cl,\,\text{sea}} - C_{Cl,f})};$$

This allows calculation of seawater contents (%) in each sample.

This seawater contribution was then used to calculate the theoretical concentration of each ion:

$$C_{i\,\text{mix}} = f_{\text{sea}}.C_{i,\text{sea}} + (1 - f_{\text{sea}}).C_{i,f}$$

These calculations take into account that Cl is a conservative tracer [37]. In fact, Cl is not usually removed from the system due to its high solubility [2]. The only inputs are either from the aquifer matrix salts or from a salinization source like seawater intrusion etc.

The PHREEQC code was used to model calcite, dolomite and gypsum saturation states of the freshwater–seawater mixing process in a closed system. This code calculated the samples ionic strength and those of the theoretical mixtures between freshwater and seawater. Moreover, PHREEQC provided the geochemical composition of these theoretical mixtures.

This software is a specialized code that uses the Mass Balance and Electroneutrality equations to simulate geochemical reactions, such as mixing of waters, addition of net irreversible reactions to solution,

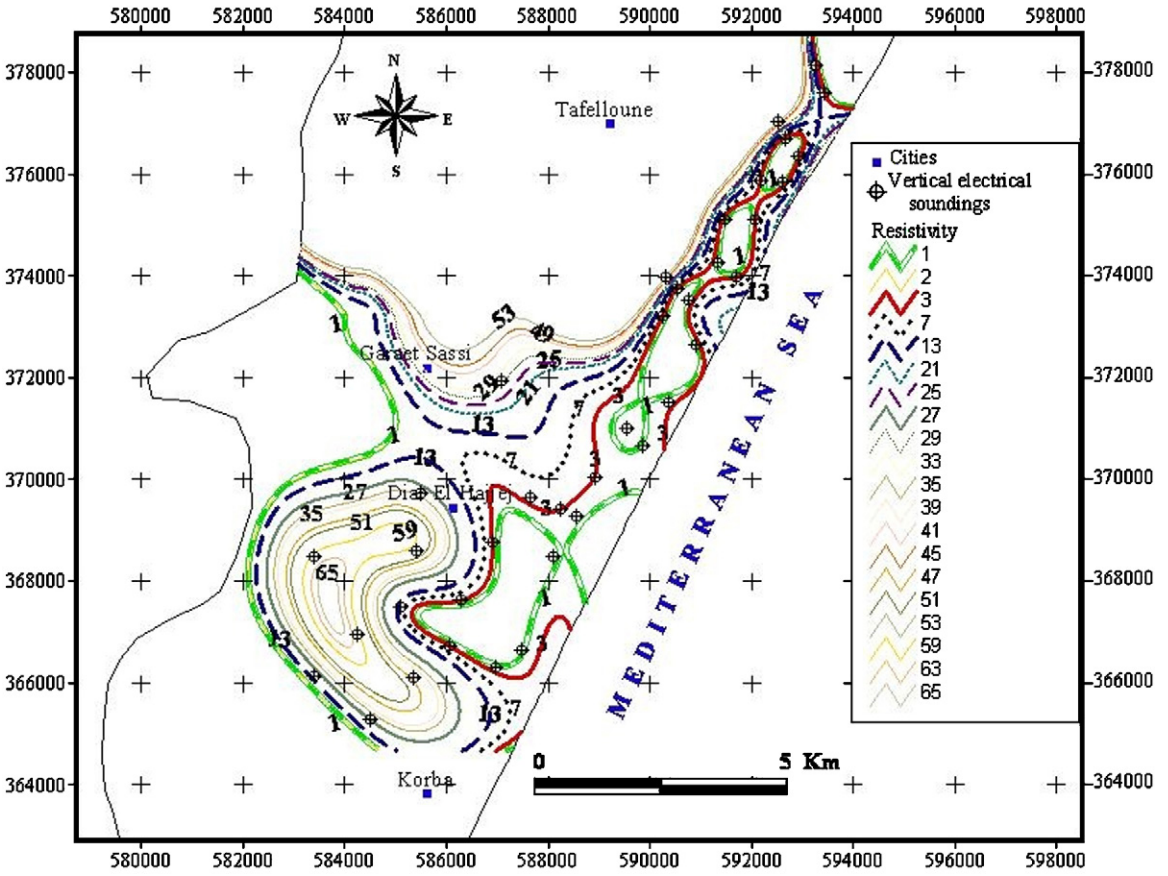

Fig. 4. Iso-resistivity contour map.

Fig. 4. Carte des contours d'iso-résistivité.

dissolving and precipitation phases to achieve equilibrium with the aqueous phase [31]. The modelled saturations states of these minerals and the geochemical compositions of mixing waters will be compared to the measured ones. This comparison would confirm the cationic exchange processes, precipitation, and mineral dissolutions.

Prior to these geochemical analyses, a geophysical survey combined to borehole logging data was applied on the study area. In fact, there is an empirical relation between the resistivity of water and its mineralization [8,25]. This geophysical method was implemented for the aquifer geometry study and the marine intrusion evaluation. In addition, the electrical resistivity of rocks depends on many factors such as groundwater salinity, saturation, aquifer lithology and porosity.

Electrical resistivity data have been used to identify the geographical extent of salinization in the aquifer, as resistivity decreases with increasing salinity. Indeed, 38 electric surveys using the Wenner process were carried out between Korba and Oued Lebna. The outcome of this geophysical survey is given below.

5. Geo-electrical study

To evaluate the extension of the marine intrusion in the coastal aquifer of the eastern coast of Cap-Bon, 38 vertical electrical soundings (VES) using the Wenner process were carried out in the area of Korba. Lines AB of these electric surveys are directed parallel to the coast. This orientation facilitates the quantitative interpretation of these electric soundings, carried out by the Winsev software. This geophysical study aims to construct an iso-resistivity map of seawater intrusion. The calibration of the VES results with borehole data enabled us to establish geological cross sections (Fig. 2), which shed more light on the geometry of the aquifer and estimate the vertical and horizontal configuration of the seawater intrusion. Thus, the main purpose of this study is to highlight the spatial distribution of the salinization and its extension.

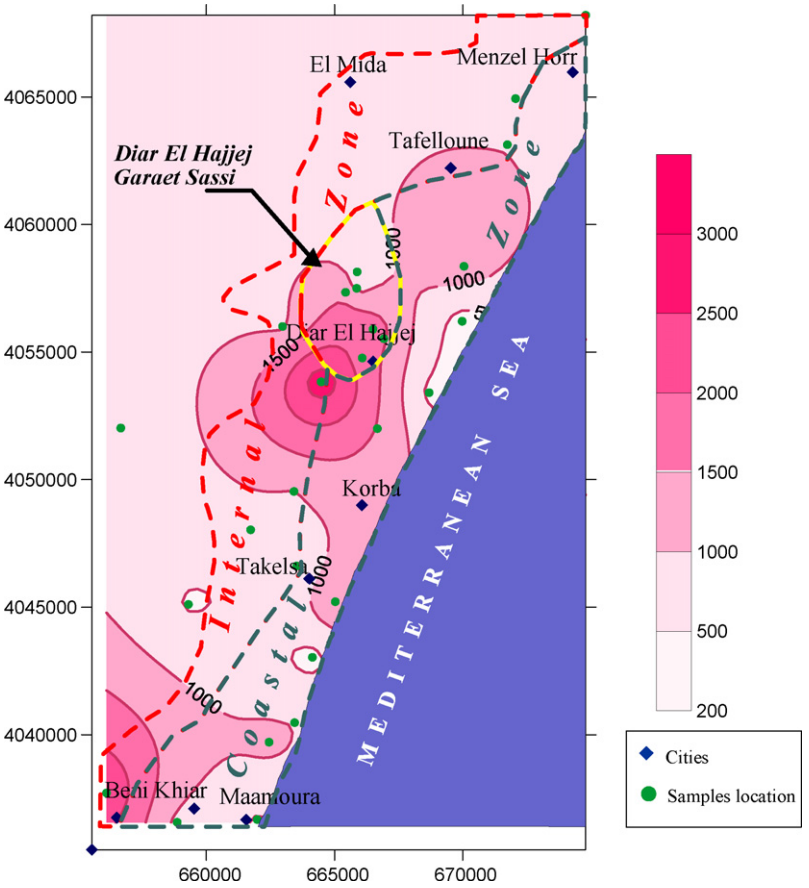

Fig. 5. Iso-chloride (ppm) contour map of Korba aquifer (June 2006).

Fig. 5. Carte des contours d'iso-valeur des chlorures (ppm) de l'aquifère de Korba.

The iso-resistivity contour map (Fig. 4) shows zones of contamination which resistivity lies between 1 to 17 Ωm. These contamination zones characterize the coastal zone and the Diar El Hajjej and Garaet Sassi areas. Some zones of relatively high resistivity located along the coast are the consequence either of the direct infiltration of rainwater through the recent littoral sandy dunes or to the rise of the substratum. This map shows the extent of the marine invasion of the area of Diar El Hajjej compared to that of Tefelloune. Given these geophysical findings, a geochemical study was undertaken and the following presents the main results and interpretations. Former studies have showed the complementarity of these two methods [6,42].

6. Hydrochemical results and discussion

Water sampling was carried out covering the Korba-Diar El Hajjej-Garaet Sassi zone and the coastal zone. The geophysical method enabled to detect low resistivities in these areas. However, during this study, we had recourse to a sampling, which exceeds these zones. This is to know the marine intrusion space extension and to do a comparison between the geochemical phenomena observed in these areas. Two samples were taken from the deep aquifer.

Water samples collected from these areas show high chloride contents (Fig. 5).The determination of the groundwater salinity origin was based on a spatial evolution of the total dissolved salt (TDS) and the major elements contents (Table 1). The high values of the TDS of water of the aquifer relate to the zones characterized by significant piezometric depressions such as the areas of Diar El Hajjej-Garaet Sassi and Korba Tazerka.

The Piper Diagram illustrates three chemical facies (Fig. 6): Na-Cl facies, Ca-Mg-Cl facies and SO_4-mixed facies. The last one characterizes one sample of the zone of Beni Khiar. The Ca–HCO_3 water type is absent. This facies characterizes the shorter residence time waters of the detritic aquifers [1].

The calculation of seawater contents (%) presents values lower than 14% of seawater.

Calcite, dolomite and gypsum SI were also calculated using the PHREEQC 2.8 software to verify

Table 1
Sampling Analytical results of Korba aquifer (June 2006) (ppm).
Tableau 1
Résultats analytiques des échantillons d'eau de l'aquifère de Korba (juin 2006) (ppm).

No.	Na^+	K^+	Ca^{2+}	Mg^{2+}	Cl^-	HCO_3^-	SO_4^{2-}	Error %	Mg/Ca	SO_4/Cl	TDS	Ionic strength
1	594	41	388	168	878	325	1557	−2.03	0.71	1.31	3951	7.36E-02
2	302	60	198	87	457	343	568	2.26	0.73	0.92	2014	3.86E-02
3	440	18	296	133	1124	412	323	0.16	0.74	0.21	2746	5.62E-02
4	518	44	219	106	983	331	438	1.16	0.80	0.33	2639	5.15E-02
5	215	24	128	45	351	308	160	4.59	0.58	0.34	1231	2.40E-02
6	979	61	240	85	1510	436	431	3.57	0.58	0.21	3741	6.98E-02
7	204	9	90	56	386	198	165	1.58	1.02	0.32	1106	2.23E-02
8	743	24	314	110	1370	360	605	0.45	0.58	0.33	3526	6.81E-02
9	437	9	333	60	983	215	490	−0.75	0.30	0.37	2528	5.07E-02
10	457	10	208	54	808	383	290	−0.24	0.43	0.26	2209	4.19E-02
11	279	4	159	103	737	285	318	−5.66	1.07	0.32	1885	3.77E-02
12	166	9	61	48	281	180	163	0.69	1.30	0.43	908	1.81E-02
13	1138	23	426	301	2458	360	872	1.43	1.16	0.26	5577	1.13E-01
14	279	212	179	90	457	459	502	4.73	0.83	0.81	2178	3.96E-02
15	391	20	216	109	843	325	316	2.23	0.83	0.28	2220	4.51E-02
16	259	16	266	127	597	354	478	4.07	0.79	0.59	2097	4.35E-02
17	849	0	346	128	1475	244	935	−0.28	0.61	0.47	3977	7.67E-02
18	340	14	136	167	843	354	229	1.81	2.03	0.20	2081	4.39E-02
19	514	18	278	269	1440	372	292	5.41	1.59	0.15	3183	7.12E-02
20	1198	112	226	270	2845	459	57	−0.25	1.97	0.01	5166	1.05E-01
21	402	15	149	143	913	343	219	1.57	1.58	0.18	2184	4.50E-02
22	337	10	173	187	878	354	203	5.62	1.78	0.17	2142	4.73E-02
23	333	12	271	201	913	267	466	5.91	1.22	0.38	2464	5.44E-02
24	560	27	470	193	1756	227	433	1.71	0.68	0.18	3666	8.01E-02
25	563	14	385	159	1545	238	356	2.00	0.68	0.17	3260	7.01E-02
26	536	12	492	199	1861	238	372	0.35	0.67	0.15	3711	8.21E-02
27	542	15	179	154	983	378	377	4.38	1.42	0.28	2628	5.30E-02
28	511	15	120	94	632	627	207	5.71	1.30	0.24	2207	3.59E-02

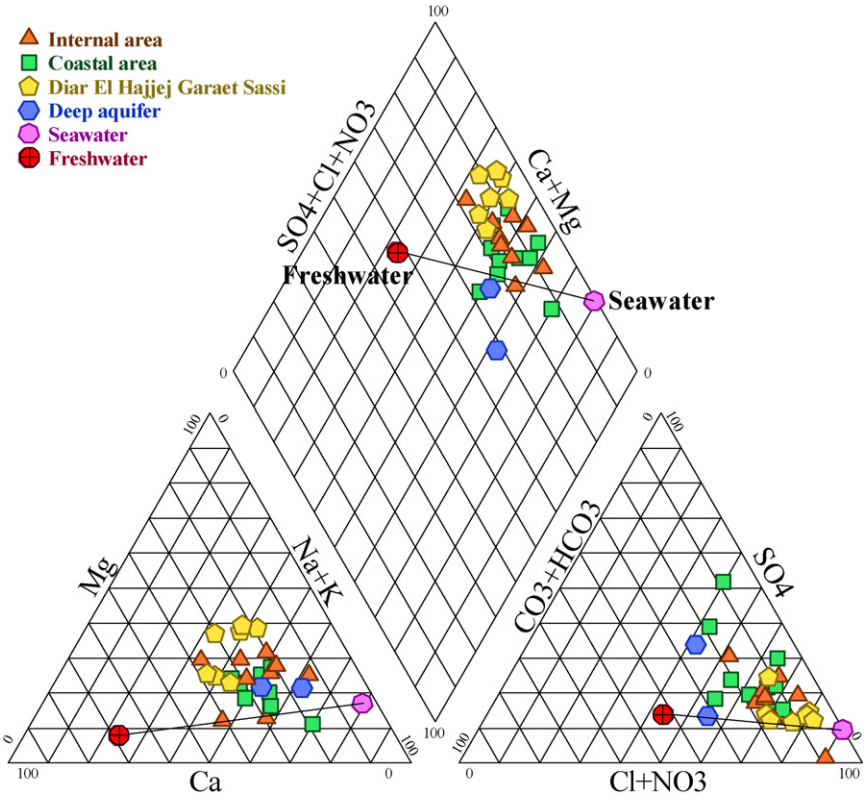

Fig. 6. Water sampling analytical results plotted in the Piper Diagram (June 2006 survey).

Fig. 6. Représentation des résultats analytiques des échantillons d'eau dans le diagramme de Piper (juin 2006).

the salinization phenomena, the exchange processes, the precipitation and dissolution of some minerals, and the dolomitization processes. Gypsum SI were modelled for different mixing rates to assess the possibility of SO_4^{2-} reduction or an alternative SO_4^{2-} source (such as gypsum dissolution). Fig. 7 shows calcite, dolomite and gypsum saturation index versus seawater in the mixture. Also shown is the theoretical line of conservative mixing.

The Mg/Ca ratios of the aquifer water are modelled by the PHREEQC software and calculated from the concentration of chlorides. According to the proportions of seawater, the Mg/Ca ratios modelled by the two methods have the same shape, which enhances the reliability of these methods for the calculation of theoretical concentrations.

The PHREEQC code was also used to calculate the ionic strength.

Debye-Hückel has proved to be remarkably successful in predicting activity coefficients in dilute solution. The extended Debye-Hückel Equation is most useful at concentrations less than 0.1 M, which includes many natural waters and provides adequate approximation for activity coefficients up to ionic strengths of about 1 M, which would include most solutions of geological interest, including seawater. The Davies equation is slightly more accurate in the range of 0.1 to 1 M ionic strength. Above these concentrations, both the Davies and Debye-Hückel equations are increasingly inaccurate [40]. The ionic strength values calculated lie between 1.81E-02 and 7.30E-01 (Table 1). The last value is that of seawater. This means that the use of the PHREEQC code is validated in the case of the explored salinity ranges.

6.1. Diar El Hajjej and Garaet Sassi

The relationship between Na^+ and Cl^- (Fig. 8a) demonstrates low Na^+ contents in these samples. In fact, the Diar El Hajjej Garaet Sassi Korba samples are positioned lower than the theoretical mixing freshwater–seawater line. These samples are especially controlled by an inverse cation exchange between Na and Ca-Mg. This behaviour is documented by a majority of samples enriched in Ca^{2+} and/or Mg^{2+} with respect to the theoretical mixture (Fig. 8b and c). Divergences from the lines could be attributed to an ion

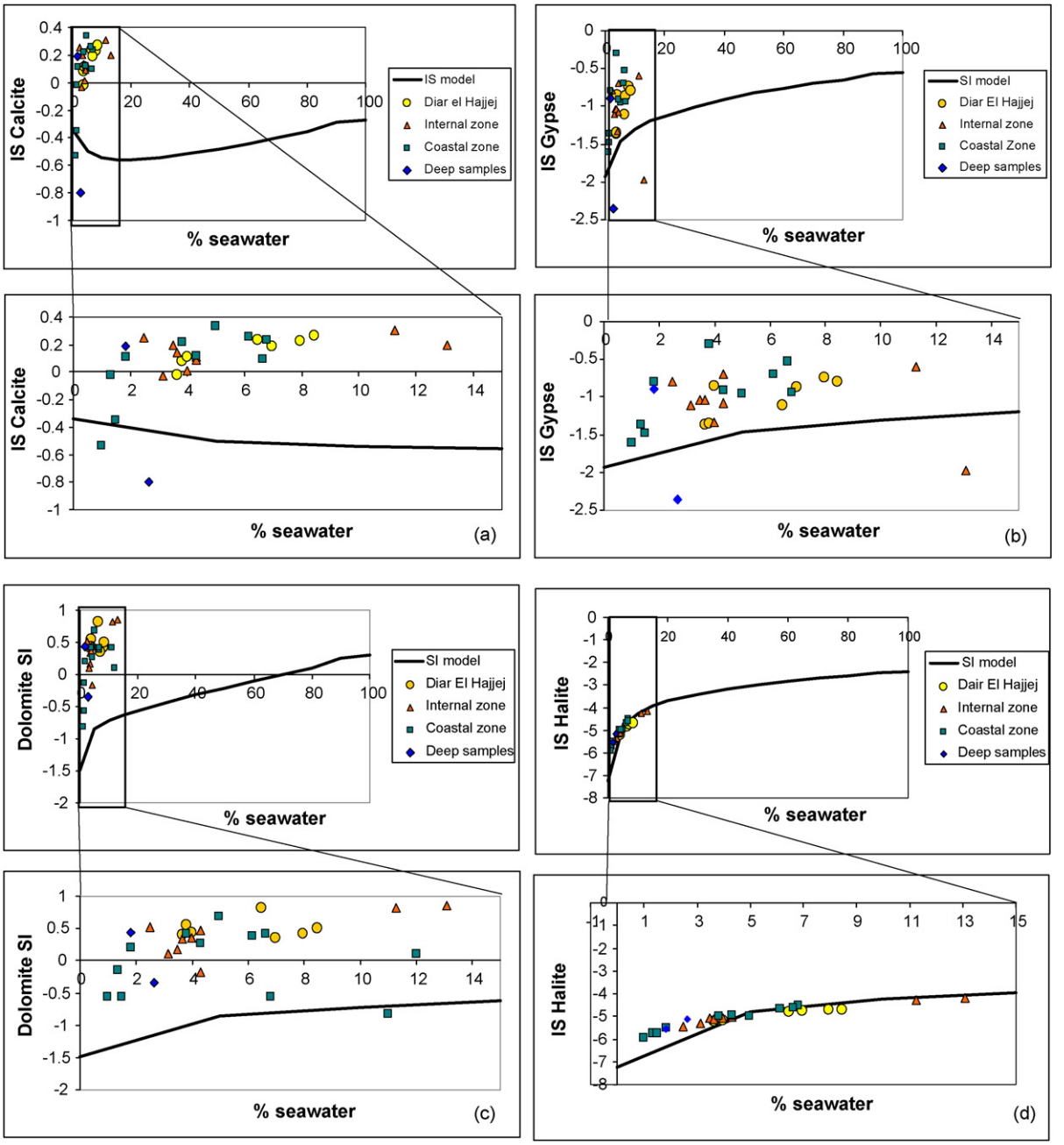

Fig. 7. SI of calcite (a), gypsum (b), dolomite (c) and halite (d) of the Korba aquifer samples. SI of the conservative mixture of freshwater and seawater.

Fig. 7. Index de saturation de la calcite (a), du gypse (b), de la dolomite (c) et de l'halite (d) dans les échantillons de l'aquifère de Korba. Index de saturation du mélange conservatif eau douce/eau de mer.

exchange phenomenon. In fact, many samples present an excess of calcium and/or Mg^{2+} and a deficit of sodium compared to chlorides. When seawater intrudes a freshwater aquifer, an inverse cation exchange occurs and sodium is captured by the exchanger (clay), while Ca^{2+} and/or Mg^{2+} is released, thus water quality changes from Na-Cl rich to $CaCl_2$-rich water and/or Mg-Cl_2[12].

This behaviour is confirmed by the calculation of ΔNa^{+}, ΔCa^{2+} and ΔMg^{2+}.

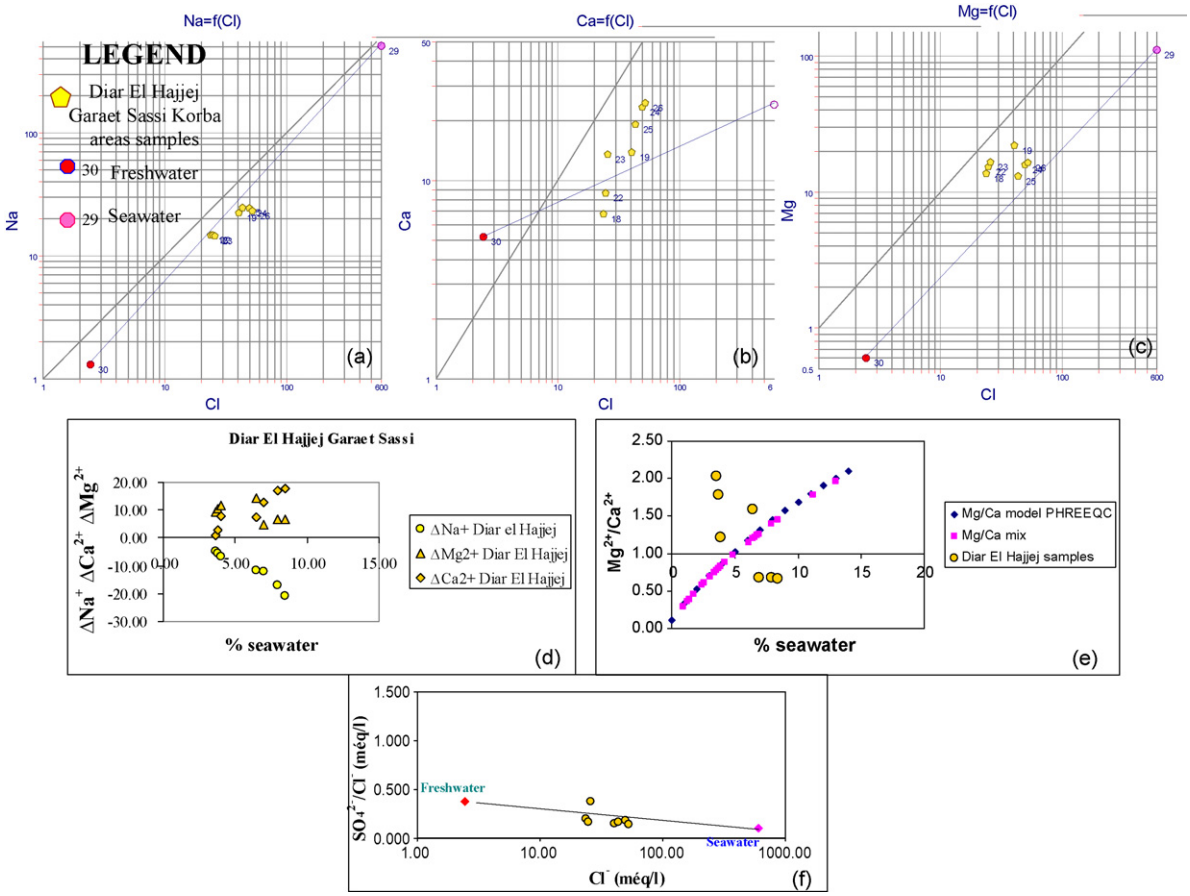

Fig. 8. Na^+, Mg^{2+}, Ca^{2+}/Cl^- relationships (meq/l) (a,b,c), ΔNa^+, ΔCa^{2+} and ΔMg^{2+} relationships with % seawater (d), Mg^{2+}/Ca^{2+} ratio relationship with % seawater (e) and SO_4^{2-}/Cl^- ratio relationship with chlorides (f) in Diar El Hajjej Garaet Sassi area (June 2006).

Fig. 8. Relations Na^+, Mg^{2+}, Ca^{2+}/Cl^- (meq/l) (a,b,c) de ΔNa^+, ΔCa^{2+} et ΔMg^{2+} avec le pourcentage d'eau de mer (d), du rapport Mg^{2+}/Ca^{2+} avec le pourcentage d'eau de mer (e) et du rapport SO_4^{2-}/Cl^- avec les chlorures (f) dans la zone de Diar El Hajjej Garaet Sassi (juin 2006).

In fact, the ΔNa^+ is usually negative and the ΔCa^{2+} and ΔMg^{2+} are positive (Fig. 8d). The most logical explanation for this excess of Ca^{2+} and Mg^{2+} is an inverse cation exchange. This confirms the mixture of freshwaters with seawater. The higher the deviation (Δ), the more important are the processes modifying the content of the mixing.

The Mg^{2+}/Ca^{2+} ratio increases proportionally to seawater in the mixture [34,38,39]. The SO_4/Cl ratio decreases as the seawater proportion in the mixture increases [34,38,39].

This seawater contamination hypothesis is conformed by the fact that the highest Mg^{2+}/Ca^{2+} ratio values (Fig. 8e) and the weakest SO_4^{2-}/Cl^- ratios (Fig. 8f) characterize the Diar El Hajjej and Garaet Sassi areas samples.

Some Diar El Hajjej area samples are characterized by low SO_4^{2-}/Cl^- ratio (between 0.148 and 0.182) and an average Mg^{2+}/Ca^{2+} ratio (between 0.668 and 0.681). This is caused by their enrichment in calcium, which originates by the inverse cation exchange between water and clays of the substratum [38].

The samples of Diar El Hajjej-Garaet Sassi areas present SI higher than the modelled values of the conservative mixture. Differences between the theoretical saturation states and the ones calculated for the samples arise due to the non-conservative nature of dissolution and precipitation of the calcite and the CO_2 flux (P_{CO_2}) [33]. The Diar El Hajjej-Garaet Sassi samples plot above the calcite SI line for the conservative mixing and all these samples are oversaturated in this mineral. These samples are oversaturated with respect to gypsum. Gypsum SI are generally higher than the theoretical conservative mixing line. This requires a source in SO_4 other than seawater like the dissolution of gypsum present in the

catchment area or the evaporation of the irrigation water excess. The dolomite SI are higher than 0.

The basic requirement for the deposition of dolomite is that the [Mg]/[Ca] ratio has to exceed 1. This condition is met in the majority of the samples. These ratios are characterized by values higher than those modelled suggesting the presence of another Mg^{2+} source different from seawater. This water reached the precipitation condition of dolomite.

The Mg/Ca ratios of three samples are lower than those modelled with proportion higher than 5% in seawater. These samples are characterized by dolomite SI > 0.This confirms the assumptions of the dolomite precipitation causing thus the Mg^{2+}/Ca^{2+} ratio reduction or the inverse cation exchange Na^{+}-Ca^{2+} and the salinization.

The halite SI follows the conservative mixing line direction. This confirms the marine origin of this mineral.

6.2. Coastal area

The Na^{+} and Cl^{-} relationship demonstrates that the coastal area samples plot above the seawater-freshwater mixture line (Fig. 9a). This is confirmed by the fact that ΔNa^{+} is positive in most samples of this area. The most logical explanation for this excess of Na^{+} is that a direct cation exchange is taking place with the clay substratum. This exchange produces Na^{+} release to the solution and Ca^{2+} and/or Mg^{2+} capture from it. This process is caused by the water flushing. Fig. 9b and c show that most of the samples plot above the mixing line. Two samples taken from the coastal zone have positive ΔNa^{+} and negative ΔCa^{2+} and/or ΔMg^{2+} (Fig. 9d). This shows the contribution of the coastal dunes to the recharge of the aquifer and the presence in this zone of clay layers playing the role of barrier against seawater intrusion.

In general, ΔNa^{+} ΔCa^{2+} and ΔMg^{2+} are positive (Fig. 9d). This confirms the hypothesis of the aquifer

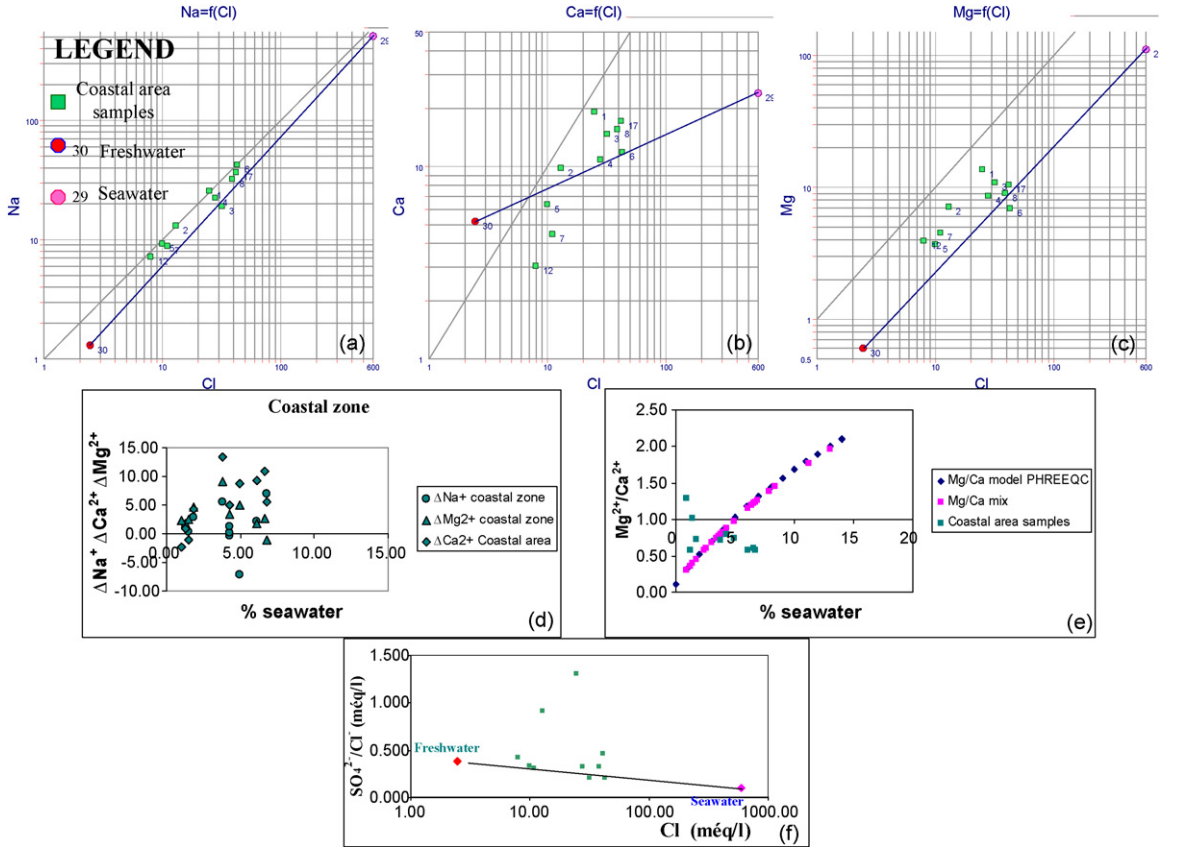

Fig. 9. Na^{+}, Mg^{2+}, Ca^{2+}/Cl^{-} relationships (meq/l) (a,b,c), ΔNa^{+}, ΔCa^{2+} and ΔMg^{2+} relationships with % seawater (d), Mg^{2+}/Ca^{2+} ratio relationship with % seawater (e) and SO_4^{2-}/Cl^{-} ratio relationship with chlorides (f) in the coastal area (June 2006).

Fig. 9. Relations Na^{+}, Mg^{2+}, Ca^{2+}/Cl^{-} (meq/l) (a,b,c) de ΔNa^{+}, ΔCa^{2+} et ΔMg^{2+} avec le pourcentage d'eau de mer (d), du rapport Mg^{2+}/Ca^{2+} avec le pourcentage d'eau de mer (e) et du rapport SO_4^{2-}/Cl^{-} avec les chlorures (f) dans la zone côtière (juin 2006).

flushing in the coastal area. The excess of Ca^{2+} and Mg^{2+} is due to the dissolution of the carbonates and the gypsum present in the catchment area and dispersed in the aquifer. This phenomenon is accompanied by a sulphate-enrichment confirming the hypothesis of gypsum dissolution. The Ca^{2+} and Mg^{2+} excesses cause the calcite, dolomite oversaturations. This is shown in the SI of these minerals calculated by PHREEQC.

Two samples only (No. 3 and 4) have negative ΔNa^{+}. These samples are located in the north of Beni Khiar. They are characterized by an inverse cation exchange.

The most coastal samples present average Mg^{2+}/Ca^{2+} and SO_4^{2-}/Cl^{-} ratios values (Fig. 9e and f). These samples are located in the coastal consolidated dunes of the Tyrrhenian. In this area, the aquifer is strongly recharged by meteoric water [14]. This confirms the water flushing theory of the aquifer in the coastal zone.

The majority of samples present SI higher than the modelled values of the conservative mixture. The basic requirement for the deposition of dolomite is that the [Mg]/[Ca] ratio exceeds 1. This condition is met only in two of these samples (No. 7 and 12). In spite of this, the dolomite and calcite SI are negative and dolomitization is not reached. This situation is due to the low salinity (TDS) of these water samples.

The gypsum and halite SI are negative but they are higher than the theoretical conservative mixing line. The behaviour of the halite SI is explained by the excess of Na^{+}. In fact, all the samples plot above the theoretical mixing line. The gypsum SI behaviour requires a source in SO_4 other than seawater like the dissolution of gypsum present in the catchment area or the evaporation of the irrigation water excess.

6.3. Internal zone and deep aquifer

The Na^{+} and Cl^{-} relationship indicates that the majority of the internal area samples approach the mixing line (Fig. 10a) indicating a weak interaction between the freshwater–seawater mixing and the substratum clay.

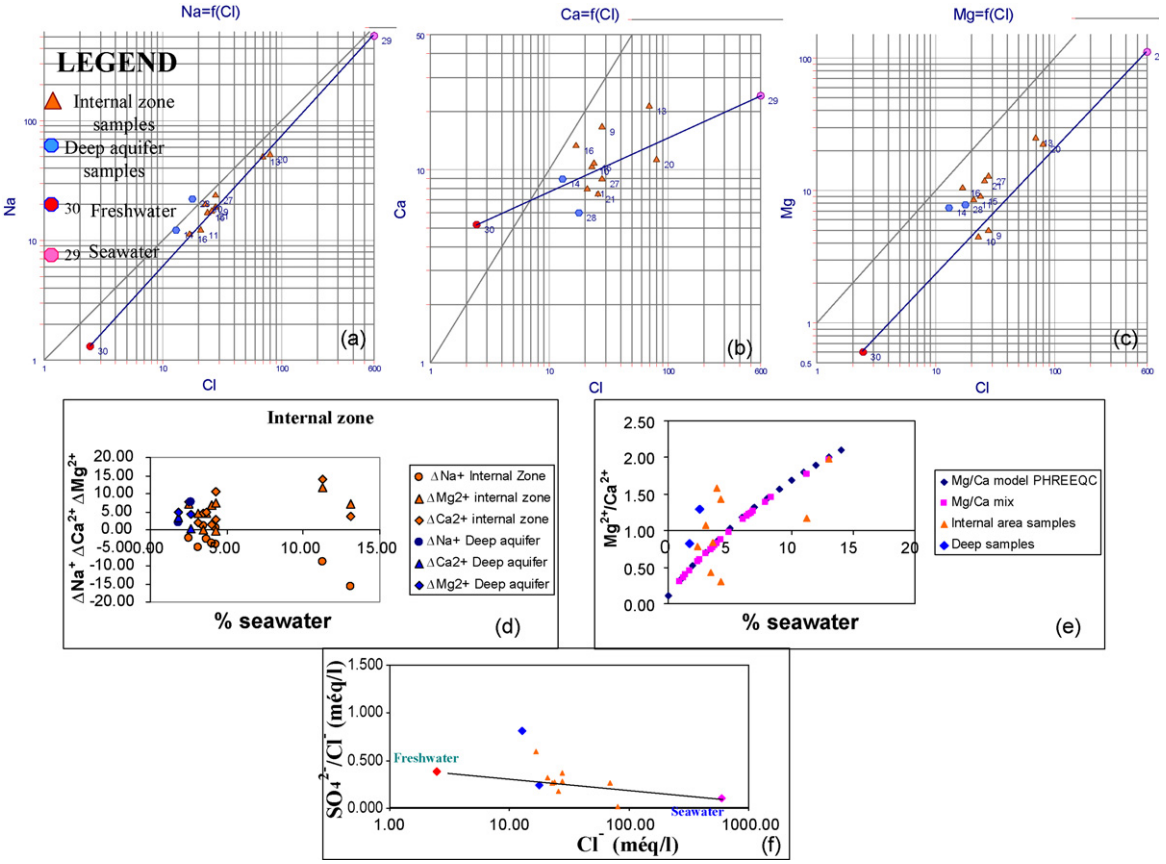

Fig. 10. Na^{+}, Mg^{2+}, Ca^{2+}/Cl^{-} relationships (meq/l) (a,b,c), ΔNa^{+}, ΔCa^{2+} and ΔMg^{2+} relationships with % seawater (d), Mg^{2+}/Ca^{2+} ratio relationship with % seawater (e) and SO_4^{2-}/Cl^{-} ratio relationship with chlorides (f) in the internal area and the deep aquifer (June 2006).

Fig. 10. Relations Na^{+}, Mg^{2+}, Ca^{2+}/Cl^{-} (meq/l) (a,b,c) de ΔNa^{+}, ΔCa^{2+} et ΔMg^{2+} avec le pourcentage d'eau de mer (d), du rapport Mg^{2+}/Ca^{2+} avec le pourcentage d'eau de mer (e) et du rapport SO_4^{2-}/Cl^{-} avec les chlorures (f) dans la zone interne et dans l'aquifère.

Fig. 10b and c show the calcium and the magnesium behaviour. These cations have the most distinctive distribution pattern in the mixing water sample and exhibit concentrations that exceed the theoretical concentrations. This is produced by the inverse exchange between Na and Ca-Mg caused by seawater intrusion and the dissolution of dolomite.

The ΔNa^+ is usually negative but these values approach 0 (Fig. 10d). This fact confirms the weak interaction between the mixture and the substratum. As an exception, samples No. 13 and 20 are characterized by negative weak ΔNa^+ values and positive ΔCa^{2+} and ΔMg^{2+} values. This is in favour with the inverse cation exchange.

ΔCa^{2+} and ΔMg^{2+} are positive in all the samples except the samples No. 9 (Fig. 10d). The probable origin of this excess of Mg^{2+} and Ca^{2+}, in addition to the inverse cation exchange, is the dissolution of the gypsum and the dolomite.

Mg/Ca is higher than 1 or near to 1 (Fig. 10e). This confirms the dolomitization phenomenon.

Only samples No. 9 and 10 have low Mg/Ca values. These values are lower than those modelled by PHREEQC and by those calculated from the Cl concentration. This resulted in weak dolomite saturations indexes. Dolomite and calcite IS are usually positive in this area. Gypsum SI are higher than those modelled. Halite SI are on the mixture line.

In the deep aquifer, the Na^+, Ca^{2+}, Mg^{2+} and Cl^- (Fig. 10a–c) relationships demonstrates that these samples plot above the seawater-freshwater mixture line. This is confirmed by positive ΔNa^+, ΔCa^{2+} and ΔMg^{2+} (Fig. 10d). This Na^+ excess is caused by a direct cation exchange with the clay present in the aquifer. This process is caused by the water flushing.

Sample No. 14 presents close Mg^{2+}/Ca^{2+} (Fig. 10e) and SO_4^{2-}/Cl^- ratios values (Fig. 10f) (respectively, 0.812 and 0.826). This is where the aquifer is recharged by meteoric water. This confirms the water flushing theory of the aquifer in this area. Calcite and dolomite SI are positive in this sample. This explains the Mg/Ca ratio reduction.

On the other hand, sample No. 28 is characterized by a high Mg^{2+}/Ca^{2+} ratio and a low SO_4^{2-}/Cl^- ratio. In spite of this, the dolomite and calcite SI are negative and dolomitization is not reached. This situation is due to the low salinity (TDS) of this water sample. The gypsum SI is negative but it is lower than the theoretical conservative mixing line.

The behaviour of the halite SI of the two samples is explained by the excess of Na^+. In fact, these SI are slightly higher than those modelled.

7. Conclusion

The aquifer of Korba shows especially high values of TDS in the coastal zones, the Diar El Hajjej, Garaet Sassi and Tazerka-Korba. These high TDS values are due to contamination by sea water. This assumption is justified by negative piezometric values, strong chloride concentrations and weak electric resistivity. In the various studied diagrams, we observe a tendency between sample composition and marine water composition, which gives an additional argument in favour of the presence of a marine intrusion in the coastal zone, areas of Diar El Hajjej, Garaet Sassi and Tazerka-Korba.

This seawater intrusion is accompanied by other processes, which modify the hydrochemistry of the coastal aquifer. The most remarkable process is that of the inverse cation exchange, characteristic of the changes of the theoretical mixture of seawater-freshwater, which is carried out between clays and the aquifer water. This exchange consists in the release of Ca^{2+} and/or Mg^{2+} and the adsorption of Na^+. This process characterizes Diar El Hajjej-Garaet Sassi and the internal areas.

The coastal zone is characterized by a low salinity and weak concentrations chloride. These low (Cl^-) values are due to the infiltration of meteoric water in the Tyrrhenian consolidated dunes [14] and to the presence of clay layers playing as a barrier against seawater intrusion (Fig. 2). Moreover, the direct cation exchange between Na^+ and Ca^{2+} and/or Mg^{2+} (Na^+ release and adsorption of Ca^{2+} and/or Mg^{2+}) indicating a local flushing of water of the aquifer is detected in this zone. This phenomenon is accompanied by a sulphate enrichment. The most probable source of sulphates is the dissolution of the gypsum dispersed in the aquifer.

Other processes such as dolomitization (dolomite precipitation) exist in this aquifer, but they are not as obvious as the cations exchange processes. Dolomitization is indicated by an Mg^{2+}/Ca^{2+} ratio higher than 1, negative values of ΔMg^{2+} and positive values of ΔCa^{2+} and dolomite SI > 0.

It is believed that due to the increased demand for freshwater in agriculture, the area of saltwater intrusion will eventually spread, particularly during dry periods. Consequently, both groundwater monitoring and management and groundwater conservation are essential for efficient surveillance of the saltwater intrusion.

References

[1] D.M Allen, M. Suchy, Results of the Groundwater Geochemistry Study on Saturna Island, British Columbia. Rapport final préparé

pour : Islands Trust Victoria, B.C. Earths Sciences Simon Fraser University, 2001.
[2] C.A.J. Appelo, D. Postma, Geochemistry, Groundwater and Pollution. Balkema, Rotterdam, 1993, 536p.
[3] B. Arfib, J. Ganoulis, Modélisation physique de l'intrusion d'eau de mer dans un aquifère karstique : cas de l'Almyros d'Héraklion (Crète), C. R. Acad. Sci. Paris, Ser IIa 336 (2004) 999–1006.
[4] B. Arfib, T. Cavalera, E. Gilli, Influence de l'hydrodynamique sur l'intrusion saline en aquifère karstique côtier, C. R. Geoscience 338 (2006) 757–767.
[5] H. Ben Salem, Notice explicative de la carte géologique de la Tunisie à 1/50.000 Menzel Bou Zelfa Feuille n° 22, 1998.
[6] M. Boughriba, A. Melloul, Y. Zarhloule, A. Ouardi, Extension spatiale de la salinisation des ressources en eau et modèle conceptuel des sources salées dans la plaine des Triffa (Maroc nord-oriental), C. R. Geoscience 338 (2006) 768–774.
[7] A. Chakroun, D. Zaghbib-Turki, A.M. Moigne, H. De Lumley, Découverte d'une faune de mammifère du Pléisticène supérieur dans la grotte d'El Geffel (Cap-Bon, Tunisie), C. R. Palevol 4 (2005) 317–325.
[8] G. De Moor, W. De Breuck, De freatische waters in het Oostelijke Kustgebied en in de Vlaamse Vallei, Natuurwet. Tijdsch. 51 (1969) 3–68.
[9] Z. Demirel, The history and evaluation of saltwater intrusion into a coastal aquifer in Mersin, Turkey, J. Environ. Manag. 70 (2004) 275–282.
[10] Direction Générale des Ressources en Eau, Annuaire d'exploitation des nappes phréatiques, 1995.
[11] F. Damak Derbel, D. Zaghbib Turki, C. Yaich, Le Pliocène marin du Cap-Bon (Tunisie) : exemple de dépôts gravitaires, Géol. Méditerranéenne tome XVIII (1991) 189–198.
[12] A. El Achheb, J. Mania, J. Mudry, Mécanismes d'acquisition de la minéralisation des eaux souterraines dans le bassin Sahel-Doukkala (Maroc occidental). Approche par des traceurs hydrogéochimiques, IGME, Madrid, ISBN, 2003, 84-7840-. 470-8.
[13] B. El Mansouri, Y. Loukili, D. Esselaoui, Mise en évidence et étude du phénomène de l'*upconing* dans la nappe côtière du Rharb (NW du Maroc), IGME, Madrid, ISBN, 2003, 84-7840-470-8.
[14] M. Ennabli, Étude hydrogéologique des aquifères du Nord-Est de la Tunisie pour une gestion intégrée des ressources en eau, Thèse Univ. Nice, 1980.
[15] E. Farber, A. Vengosh, I. Gavrieli, A. Marie, T.D. Bullen, B. Mayer, R. Holtzman, M. Segal, U. Shavit, The origin and mechanisms of salinization of the Lower Jordan River, Geochim. Cosmochim. Acta 68 (2004) 1989–2006.
[16] M.D. Fidelibus, Environmental tracing in coastal aquifers: old problems and new solutions, in: Coastal Aquifers Intrusion Technology: Mediterranean Countries, vol. II, Publ. IGME, Madrid, 2003, pp. 79–111.
[17] R.A. Freeze, J.A. Cherry, Groundwater, Prentice-Hall, Englewood Cliffs, NJ, 1979.
[18] N. Gaaloul, H. Alexander, D. Cheng, Hydrogeological and hydrochemical investigation of Coastal Aquifers in Tunisia-Crisis in overexploitation and salinisation, Second International Conference on Saltwater Intrusion and Coastal Aquifers-Monitoring, Modeling and Management, Merida, Mexico, March 30-April 2, 2003.
[19] K. Gemail, A. Samir, C. Oelsner, S.E. Mousa, S. Ibrahim, Study of saltwater intrusion using 1D, 2D and 3D resistivity surveys in the coastal depressions at the eastern part of Matruh area, Egypt, EAGE 2 (2004) 103–109.
[20] S. Grassi, G. Cortecci, Hydrogeology and geochemistry of the multilayered confined aquifer of the Pisa plain (Tuscany – central Italy), Applied Geochemistry 20 (2004) 41–54.
[21] C. Güler, G.D. Thyne, J.E. McCray, A.K. Turner, Evaluation of graphical and multivariate statistical methods for classification of water chemistry data, J. Hydrogeol. 10 (2002) 455–474.
[22] P. Hudak, Sulfate and chloride concentrations in Texas aquifers, J. Environ. Int. 26 (2000) 55–61.
[23] U. Kafri, A. Arad, Current Subsurface intrusion of Mediterranean seawater. A possible source of groundwater salinity in the rift valley system, Israel, J. Hydrol. 44 (1979) 267–287.
[24] S. Krimissa, J.L. Michelot, L. Bouchaou, J. Mudry, Y. Hsissou, Sur l'origine par altération du substratum schisteux de la minéralisation chlorurée des eaux d'une nappe côtière sous climat semi-aride (Chtouka-Massa, Maroc), C. R. Acad. Sci. Paris, Ser. IIa 336 (2004) 1363–1369.
[25] L. Lebbe, K. Walraevens, P. Van Burm, W. De Breuck, L'évolution de la distribution des eaux douces et salées dans la nappe libre de la plaine maritime aux environs de la frontière belgo-française, Ann. Soc. Géol. Nord, CIX (1989) 55–65.
[26] F.S. Martos, P.A. Bosch, L.M. Sanchez, A. Angela Vallejos-Izquierdo, Identification of the origin of salinization in groundwater using minor ions Lower Andarax, Southeast Spain, Sci. Tot. Environ. 297 (2001) 43–58.
[27] S.B. Olobaniyi, F.B. Owoyemi, Characterization by factor analysis of the chemical facies of groundwater in the deltaic plain sands aquifer of Warri, western Niger Delta, Nigeria, AJST Sci. Eng. Ser. 7 (2006) 73–81.
[28] A. Ozer, R. Pskoff, P. Sanlaville, A. Ulzega, Essai de corrélation du Pléistocène supérieur de la Sardaigne et de la Tunisie, C. R. Acad. Sci. Paris, Ser. D 291 (1980) 801–804.
[29] J.G. Paine, Determining salinization extent. Identifying salinity sources and estimating chloride mass using surface borehole and airborne electromagnetic induction methods, Water Resour. Res. 3 (2003), p. 3-1-3-10.
[30] C. Paniconi, I. Khlaifi, L. Giuditta, A. Giacomelli, J. Tarhouni, Modeling and analysis of Seawater Intrusion in the coastal aquifer of eastern Cap-Bon, Tunisia, Kluwer Academic Publishers, Netherlands, Transport in Porous Media 43, 2001, pp. 3–28.
[31] D.L. Parkhurst, C.A.J. Appelo, User's guide to PHREEQC (version 2)-A computer program for speciation, batch-reaction, one-dimensional transport, and inverse geochemical calculations, U.S. Geological Survey Water-Resources Investigations Report 99-4259, 1999, 312 p.
[32] C.P. Petelas, I.B. Diamantis, Origin and distribution of saline groundwater in the Upper Miocene aquifer system, coastal Rhodope area, northern Greece, J. Hydrogeol. 7 (1999) 305–316.
[33] P. Pulido-Lebœuf, Seawater intrusion and associated processes in a small coastal complex aquifer (Castell de Ferro, Spain), Applied Geochemistry 19 (2004) 1517–1527.
[34] P. Pulido-Leboeuf, A. Pulido-Bosch, M.L. Calvache, A. Vallejos, J.M. Andreu, Strontium, SO_4^{2-}/Cl^- and Mg^{2+}/Ca^{2+} ratios as tracers for the evolution of seawater into coastal aquifers: the example of Castell de Ferro aquifer (SE Spain), C. R. Geoscience 335 (2003) 1039–1048.
[35] E. Sanz Escudé, Brackish springs in coastal aquifers and the role of calcite dissolution by mixing waters: PhD Thesis, Department of Geotechnical Engineering and Geo-Sciences (ETCG), Technical University of Catalonia (UPC), Institute of Earth Sciences "Jaume Almera" CSIC, 2007.
[36] R.M. Spechler, Saltwater intrusion and quality of water in Floridian aquifer system, Northeastern Florida: U.S. Geological

Survey Water-Resources Investigations, Report 92-4174, 1994, 76 p.

[37] J.H. Tellam, Hydrochemistry of the saline groundwaters of the lower Mersey Basin Permo-Triassic sandstone aquifer, UK, J. Hydrol. 165 (1995) 45–84.

[38] R. Trabelsi, M. Zaïri, H. Smida, H. Ben Dhia, Salinisation des nappes côtières : cas de la nappe nord du Sahel de Sfax, Tunisie, C. R. Geoscience 337 (2005) 515–524.

[39] A. Vengosh, E. Rosenthal, Saline groundwater in Israel: its bearing on the water crisis in the country, J. Hydrol. AMST 156 (1994) 389–430.

[40] W. M. White Geochemistry, International Mine Water Association, 2005, 700 p.

[41] S.R. Wilson, M. Ingham, J.A. McConchie, The applicability of earth resistively methods for saline interface definition, J. Hydrol. 316 (2006) 301–312.

[42] L. Zouhri, E. Carlier, B. Ben Kabbour, E.A. Toto, C. Gorini, B. Louche, Groundwater interaction in the coastal environment: hydrochemical, electrical and seismic approaches, Bull. Eng. Geol. Environ. 67 (2008) 123–128. , doi:10.1007/s10064-007-0101-6.